

Exploring the origin of degenerate doublet bands in ^{106}Ag

N. Rather,¹ P. Datta,^{2,*} S. Chattopadhyay,¹ S. Roy,³ S. Rajbanshi,¹

A. Gowsami,¹ G. H. Bhat,⁴ J. A. Sheikh,⁴ R. Palit,⁵ S. Pal,⁵

S. Saha,⁵ J. Sethi,⁵ S. Biswas,⁵ P. Singh,⁵ and H. C. Jain⁵

¹*Saha Institute of Nuclear Physics, Kolkata-700064, INDIA*

²*Ananda Mohan College, Kolkata-700009, INDIA*

³*Tata Institute of Fundamental Research, Mumbai-400005, INDIA*

⁴*Department of Physics, University of Kashmir, Srinagar-190006, INDIA*

⁵*Tata Institute of fundamental Research, Mumbai-400005, INDIA*

(Dated: March 8, 2021)

Abstract

The electromagnetic transition probabilities of the excited levels for the two nearly degenerate bands of ^{106}Ag have been measured using the Doppler Shift Attenuation Method. A comparison with the calculated values using triaxial projected shell model approach indicates that these bands originate from two different quasi-particle configurations but constructed from the same mean-field deformation.

arXiv:1310.7731v1 [nucl-ex] 29 Oct 2013

In the last decade, a number of nearly degenerate pairs of rotational bands with same parity have been reported in nuclei of mass $A \sim 130$ [1–3] and $A \sim 100$ [4–7] regions. These bands are known to be strongly connected to each other and it has been proposed that a possible reason for the occurrence of these doublet bands is spontaneous breaking of chiral symmetry in triaxial nuclei due to the presence of three orthogonal angular momenta of the valence protons, valence neutrons and the core [8, 9]. However, for the two bands to be chiral partners, the near degeneracy in level energy and spin is a necessary but not a sufficient condition [10]. In addition, these bands should exhibit nearly similar moment of inertia, quasi-particle alignment, signature staggering behaviour and, more importantly, the transition probabilities.

Indeed the nuclei of ^{134}Pr [1, 2] and ^{104}Rh [4], show the closest degeneracy in energy in the observed doublet bands over a wide angular momentum domain. However, in both cases the quasi-particle alignment behaviour has been found to be different which indicates different shapes associated with the two bands. This has been supported by dissimilar behaviour of the measured $B(E2)$ rates in the two bands of ^{134}Pr [11] which rules out the possibility of static chirality. The experimental transition rates could, however, be reproduced within an interacting boson-fermion-fermion model (IBFFM) framework by assuming a triaxial equilibrium deformation with fluctuation in shape around this value. Such a model would imply that the nuclear system will fluctuate between chiral and achiral configurations [11].

An alternate view on the origin of doublet bands has emerged based on the framework of the tilted axis cranking (TAC) model complemented by the random phase approximation (RPA) and its success in describing the experimental data in $^{135,136}\text{Nd}$ [12, 13]. In this model, the doublet bands correspond to zero RPA phonon and the one RPA phonon configurations, respectively. The lowest RPA phonon energy accounts for the energy difference between the two bands near the band head and originates due to fluctuation in the orientation of shape perpendicular to the plane of neutron and proton angular momenta. Such chiral vibrations decreases with increasing angular momentum which results in the decrease of energy spacing between the doublet bands. This situation has been realized in ^{128}Cs [14] and ^{135}Nd [12] which may indicate the onset of chiral rotation at high spins. In both these nuclei, the transition rates for the doublet have been measured to be very similar and thus, are considered as the best candidates for chiral partner bands.

This picture opens up the possibility of a shape transformation in a γ -soft nucleus due

to the chiral vibrations. In this case, the shape corresponding to the main band can be quite different from its partner band (one phonon configuration). The experimental data on the doublet bands in ^{106}Ag has been interpreted in this way where the possible deformation parameters for the main and the partner bands were found to be $(\beta, \gamma) = (0.12, 28^0)$ and $(0.20, 0^0)$, respectively, from total routhian surface (TRS) calculations [5]. This picture gives an intuitive explanation for the existence of doublet bands with different moments of inertia and quasi-particle alignment behaviour.

In a recent publication [15], Ma *et al.* have proposed that the doublet bands in ^{106}Ag may originate due to two different quasi-particle structures, namely $\pi(g_{9/2})^1 \otimes \nu(h_{11/2})^1$ for the main and $\pi(g_{9/2})^1 \otimes \nu(h_{11/2})^3$ for the partner band. However, the band crossing at $I = 18 \hbar$ predicted by the Cranked Nilsson Strutinsky (CNS) calculations, is substantially higher than the observed crossing at $14 \hbar$. In addition, a preliminary B(E2) transition rates measurement [16] has been cited by Ma *et al.*. These reported B(E2) values for partner band has large uncertainty of $\gtrsim 50\%$. This measurement is consistent with both CNS prediction with fixed K value of 6 as well as with the previous interpretation [5] of triaxial and axial prolate shapes of for the doublets. In addition, no B(M1) value has been reported which is essential to determine the quasi-particle structure of the doublet bands. Thus, the previous investigations [5, 15] on the origin of the doublet bands of ^{106}Ag have indicated two contrasting possibilities namely, distinct shapes or distinct quasi-particle structures.

In order to resolve this issue, we report the first accurate measurement of transition rates in the doublet bands of $A \sim 100$ region in ^{106}Ag . The observed transition rates of the two bands have been compared with the prediction of microscopic triaxial projected shell model (TPSM) [17]. This model uses angular momentum projection technique to restore the rotational symmetry. Thus, it provides the transition probabilities between states with well defined angular momentum. It is shown that doublet bands originate from two different one-proton plus one-neutron quasi-particle structures but arising from the same mean-field deformation.

The 68 MeV ^{14}N beam from the 14-UD Pelletron at TIFR was used to populate the excited states of ^{106}Ag through $^{96}\text{Zr}(^{14}\text{N}, 4n)$ reaction. The 1 mg/cm² thick enriched ^{96}Zr target had a ^{206}Pb backing of 9 mg/cm². The γ rays were detected in Indian National Gamma Array (INGA) [18], which consisted of 20 Compton suppressed clover detectors. Two and higher fold coincidence data were recorded in fast digital data acquisition system

based on Pixie-16 modules of XIA LLC [19]. The time stamped data was sorted in a γ - γ cube and three angle dependent γ - γ matrices using the Multi-PARAmeter time stamped based Coincidence Search program (MARCOS), developed at TIFR.

The cube was analysed using the RADWARE program LEVIT8R [20] to construct the level scheme of ^{106}Ag and to determine the relative intensities of γ -rays which don't exhibit any lineshapes. The deduced level structure for the doublet bands was found to be consistent with the reported level scheme [5]. The partner band was extended to $I^\pi = 21^- \hbar$ through the addition of a 767 keV M1 transition. The crossover E2 transition of 1500 keV was also observed.

The angle dependent γ - γ matrices were constructed by placing the gamma energies detected at specific angle (40° , 90° and 157°) along one axis while the coincident γ energy was placed on the other axis. The lineshapes were observed in γ -gated spectra for both E2 and M1 transitions above $I^\pi = 12^- \hbar$ and $14^- \hbar$ for the main and the partner bands, respectively. The relative intensities of these γ rays were obtained from the gated spectrum at 90° which were normalized with the intensities of the transitions of the same multi-polarity which have been estimated from the cube. The B(M1)/B(E2) values obtained from the relative intensities for the two bands matched with the previously reported values [5] within $\pm 1 \sigma$.

The lifetimes were measured at forward and backward angles by fitting the experimental lineshapes with the theoretical lineshapes derived from the code LINESHAPE by Wells and Johnson [21]. The codes were used to generate the velocity profile of the recoiling nuclei at 40° and 157° with respect to the beam direction using the Monte Carlo technique with a time step of 0.001 ps for 5000 histories. Northcliff and Shilling [22] stopping powers formula with shell correction was used for calculating the energy loss of the recoiling ^{106}Ag nuclei in ^{206}Pb backing. The detailed procedure for lineshape fitting is described in ref. [23, 24].

For the main band, the effective lifetimes for the 18^- and 19^- levels were found by fitting the lineshapes for 1309 ($19^- \rightarrow 17^-$) and 1300 ($18^- \rightarrow 16^-$) keV γ -transitions by assuming 100% side-feed. The top feed lifetime for 17^- level was assumed to be the intensity weighted average of the lifetimes for 18^- and 19^- levels since this level is fed by both 674 ($18^- \rightarrow 17^-$) and 1309 keV γ rays. The side feeding intensity at this level was fixed to reproduce the observed intensity pattern at 90° with respect to the beam direction. In this way each lower level was added one by one and fitted until all the observed lineshapes for 1206 ($16^- \rightarrow 14^-$), 1146 ($15^- \rightarrow 13^-$), 1042 ($14^- \rightarrow 12^-$) and 979 ($13^- \rightarrow 11^-$) γ rays were included into a global

fit where only the in-band and feeding lifetimes were allowed to vary. This procedure was repeated for 157^0 . The lifetime for the 12^- level was measured by fitting the lineshape of 833 ($12^- \rightarrow 10^-$) keV γ ray extracted from the top gate of 490 keV. This was done to avoid the large feed to this level from other non-yrast states. In this case, the observed lineshape was fitted by taking into account the complete top cascade but no side feeding at 12^- level was considered. The uncertainties in the measured lifetimes were derived from the behaviour of χ^2 fit in the vicinity of the minimum.

All these levels decay by M1 transitions and their lineshapes were also fitted following the same prescription except for 490 ($13^- \rightarrow 12^-$) and 489 ($12^- \rightarrow 11^-$) keV γ rays since their lineshapes overlapped. Thus, the final values for the level lifetimes were obtained by taking the averages from the fits at the two angles and for the two de-exciting transitions. The corresponding uncertainty in a level lifetime has been calculated as the average of the uncertainties for the independent lifetime measurements for that level added in quadrature.

The same method of analysis was followed for the levels of the partner band. The 12^- level lifetime was extracted from 326 keV M1 transition since the corresponding lineshape of cross-over E2 transition of 597 keV could be contaminated due to the presence of Ge($n, n'\gamma$) reaction.

The examples of the lineshape fits in ^{106}Ag are shown in Fig. 1. The B(M1) and B(E2) transition rates have been extracted from the measured level lifetimes and are tabulated in Table I. The error bars on the values include the uncertainties on lifetime and intensity measurements added in quadrature. The measured rates are also plotted as a function of angular momentum in Fig. 2.

It is observed from Fig. 2 (a) that within the experimental uncertainty, the B(E2) rates for the two bands are essentially same. This observation is in contradiction to the preliminary results quoted in Ref. [15] which reported substantially larger B(E2) rates in the partner band. The present experimental data do not support the existing two explanations [5, 15] for the origin of the doublet bands in ^{106}Ag since, in both the cases the B(E2) rates in the partner band are expected to be two times stronger than that in the main band.

The B(M1) behaviour of the two bands are different as observed from Fig. 2 (b). The values for the partner band exhibits staggering whose phase inverts around $I^\pi = 17^- \hbar$. This staggering is absent for the main band. It may also be noted that the B(M1) value shows a dip and a peak at $I^\pi = 17^- \hbar$ for the main and partner band, respectively. Such differences

in B(M1) values would indicate two different quasi-particle structures for the two bands.

We have compared the experimental transition rates of the two bands with the predictions of TPSM. It is to be noted that this model has been successful in describing the chiral band structure and transition rates in ^{128}Cs [25] and the level structure and branching ratios of the doublet bands in ^{108}Ag [7]. For the present case of ^{106}Ag , the deformation parameters for the triaxial Nilsson potential used are $\epsilon = 0.15$ and $\gamma = 30^\circ$. This parameter set is consistent with the previous TRS calculation [5] and observed systematic of Ag-isotopes [26]. For ^{106}Ag , the nearly degenerate lowest two projected bands are found to have $K = 4$ and 2 for $\pi(g_{9/2})^1 \otimes \nu(h_{11/2})^1$ configuration. These bands are obtained from angular-momentum projection of the triaxial deformed Nilsson intrinsic states. The projected states are, therefore, constructed from the same mean-field deformation. The $K = 2$ band is ~ 0.5 MeV higher at low spins ($4\hbar$ - $12\hbar$) but becomes nearly degenerate with $K = 4$ bands around $I = 14\hbar$ which interestingly is the observed band crossing spin for the doublet. These bands originate from different quasi-particle states and the Nilsson triaxial quasi-particle energies for $K = 4$ and $K = 2$ bands were found to be 1.76 and 2.12 MeV, respectively.

In the second stage of the TPSM study, the projected bands are employed to diagonalise the shell model Hamiltonian consisting of pairing and quadrupole-quadrupole interaction terms [17]. The energies for the doublet bands following diagonalisation, are shown in Fig. 3(a). It is quite evident from the figure that calculated values are in good agreement with the experimental data and the band crossing spin is also been reproduced. It is to be noted that the CNS calculations [15] which assumes a four quasi-particle structure for the partner band does not predict this crossing correctly.

The calculated amplitude probabilities of the wavefunctions (a_{ik}^2) for the main and the partner bands are plotted in Fig. 3(b) and (c) as a function of spin. It is observed from the figure that at low spins, the main band predominantly originates from $K = 4$ (1.76 MeV) configuration while the partner band originates from $K = 2$ (2.12 MeV) configuration. At higher spins ($I \geq 15\hbar$), the partner band is pushed lower than the main band with $K=4$ configuration due to the large overlap of the degenerate $K = 2$ and 4 bands with same quasi-particle structure.

It is known that transition probabilities are very sensitive to the wavefunctions and in order to confirm the above predicted two quasi-particle structures for the doublet bands, it is quite important to compare the TPSM calculated transition probabilities with the observed

values. The comparison is shown in Fig. 2 and it is evident that experimental B(E2) transition rates for the doublet bands are in good agreement with the predicted values. The observed drop at $I = 16 \hbar$ is due to the crossing between the doublet bands which leads to the loss of collectivity. The TPSM calculations also reproduce the observed variations of B(M1) rates as function of spin for the doublet bands which are sensitive to their intrinsic quasi-particle configurations.

In summary, the level lifetimes of doublet bands have been reported for the first time in A~100 region for ^{106}Ag . The previous works proposed that these bands correspond to two different shapes (triaxial and axial prolate) which originate due to γ -softness [5] or two different quasi-particle structures, $\pi(g_{9/2})^1 \otimes \nu(h_{11/2})^1$ and $\pi(g_{9/2})^1 \otimes \nu(h_{11/2})^3$ [15]. However, the observation of very similar B(E2) rates in the two bands is inconsistent with these interpretations. The good agreement between the measured and the calculated transition rates obtained using TPSM, indicate that the doublet bands correspond to same mean-field triaxial shape but originate from different quasi-particle configurations arising from $\pi(g_{9/2})^1 \otimes \nu(h_{11/2})^1$. These calculations also reproduce the crossing between the main and partner bands at $I = 14\hbar$.

Thus, the present measurement of transition probabilities in doublet bands of ^{106}Ag opens up the possibility that these bands in A~100 region and probably in other mass regions may originate from different quasi-particle configurations. The lifetime measurements of the other observed doublet bands and a detailed study using the TPSM is highly desirable to explore this possibility.

Authors would like to thank the technical staff of TIFR-BARC pelletron facility for its smooth operation throughout the experiment. The help and cooperation of members of the INGA collaboration for setting up the array are acknowledged. This work was partially funded by the Department of Science and Technology, Government of India (No. IR/S2/PF-03/2003-III). N. Z. and P. D. (grant no. PSW-26/11-12) would also like to thank UGC for research support.

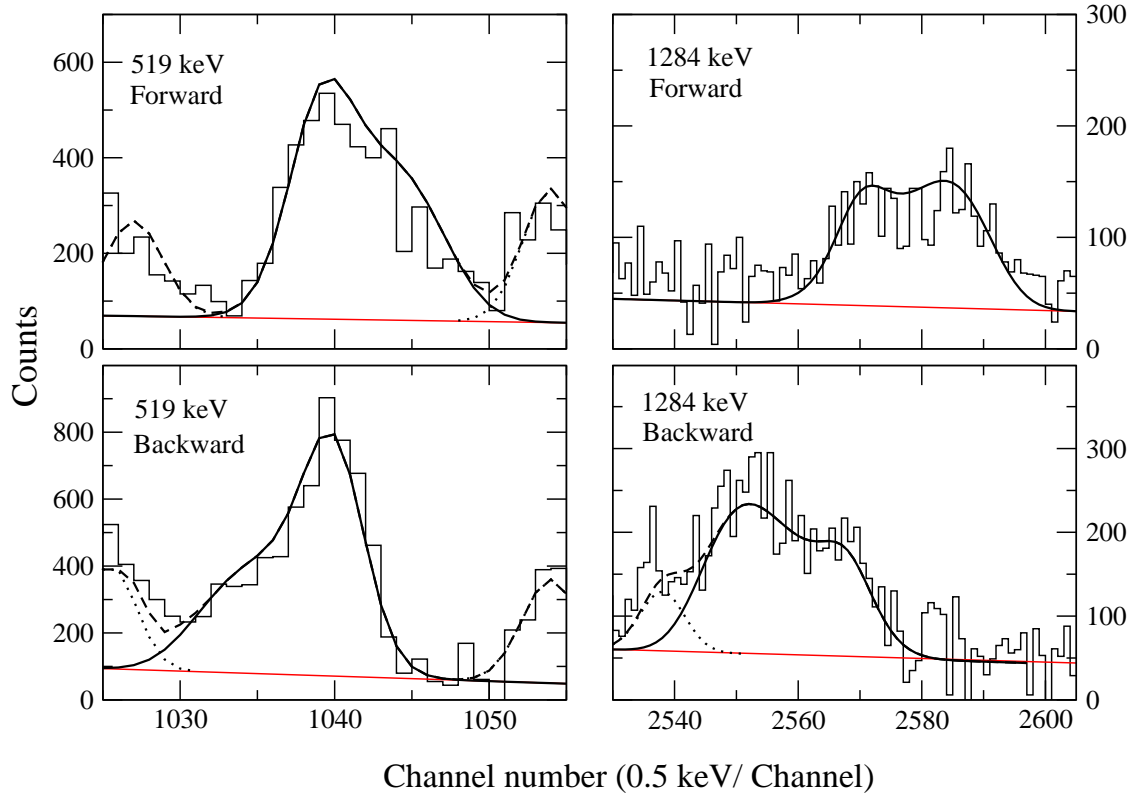


FIG. 1. Examples of the lineshape fits for 1284 ($19^- \rightarrow 17^-$) keV and 519 ($17^- \rightarrow 16^-$) keV transitions at 40° and 157° with respect to the beam direction. The Doppler broadened lineshapes are drawn in solid lines while the contaminant peaks are shown in dotted lines. The result of the fit to the experimental data is shown in dashed lines.

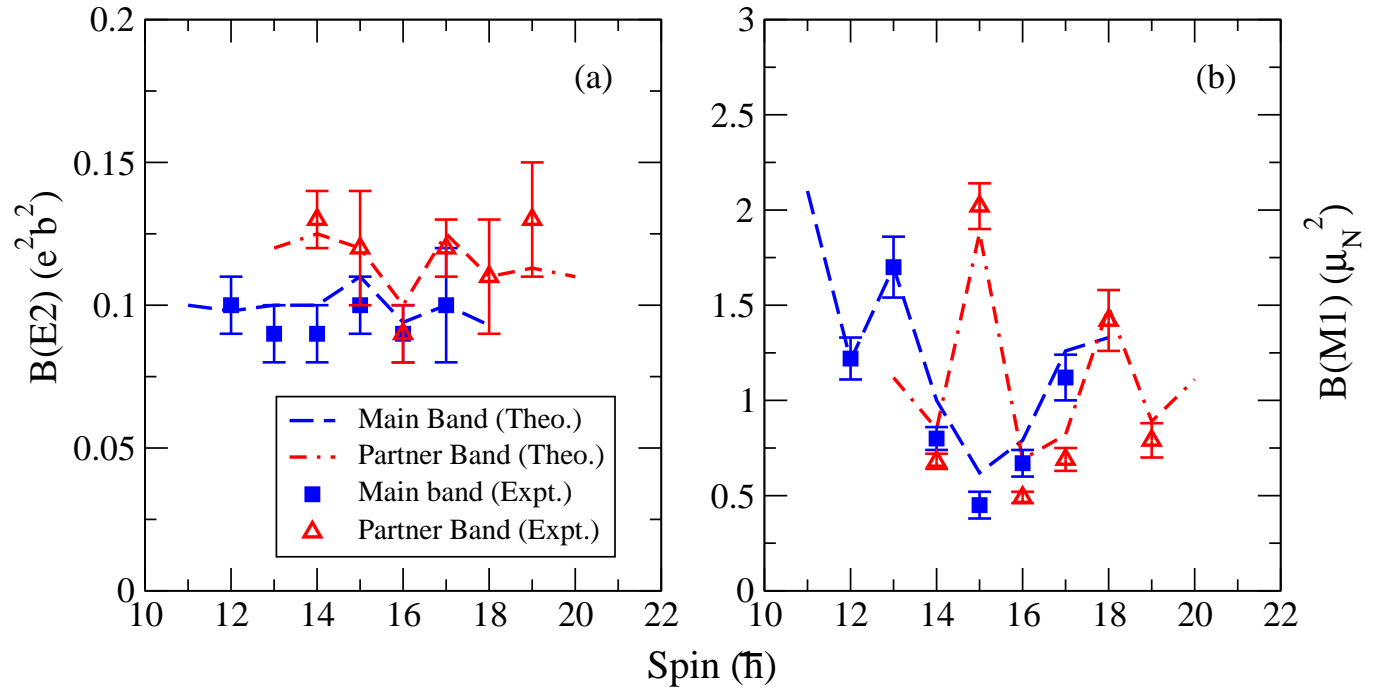


FIG. 2. Calculated and measured $B(E2)$ (a) and $B(M1)$ (b) rates for the doublet bands of ^{106}Ag . Error bars on measured values of a given level include errors in intensity and lifetime of the level added in quadrature.

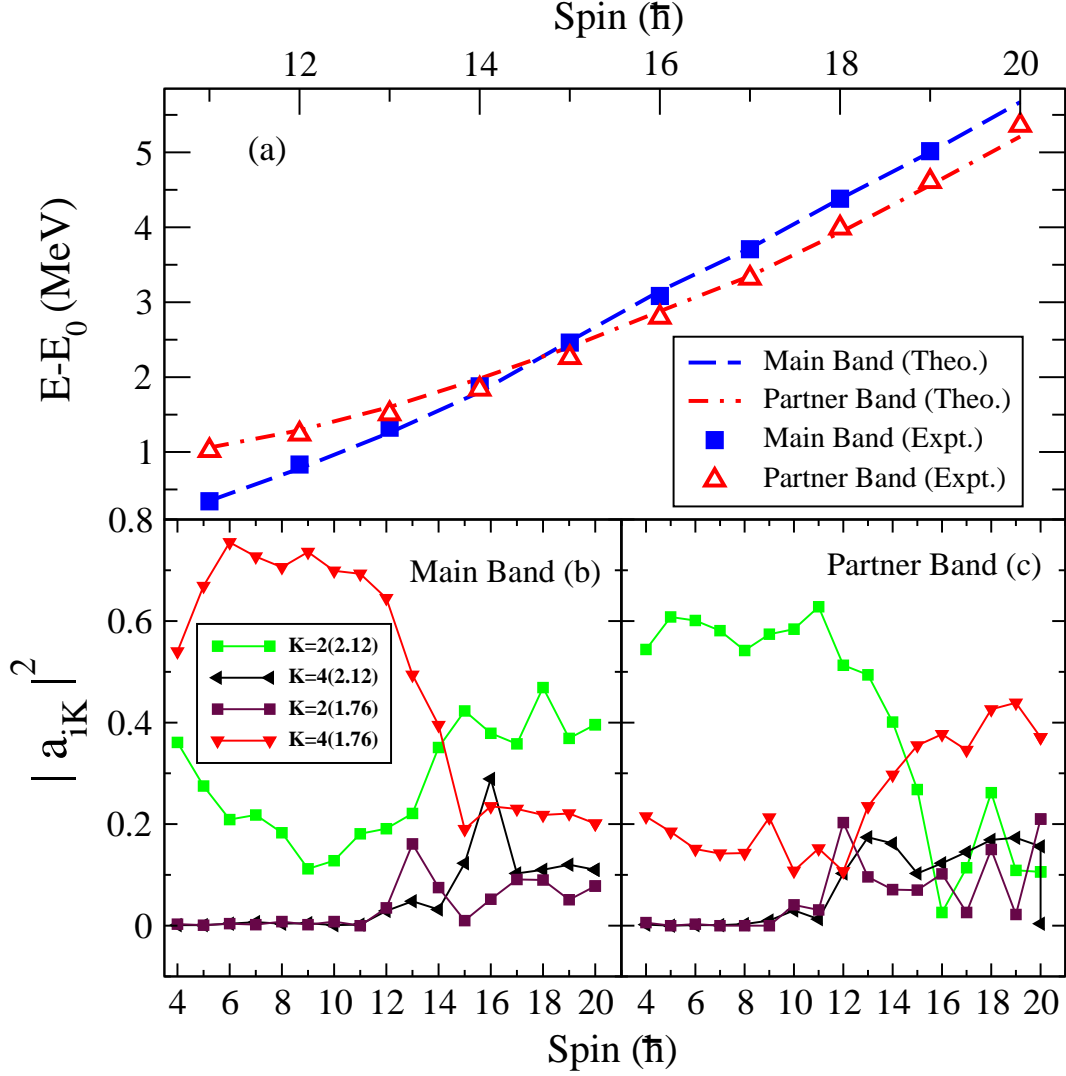


FIG. 3. (a) Comparison of the measured energy levels of negative parity doublet bands of ^{106}Ag with those from TPSM calculation. The energies are relative to the band head E_0 taken to be the energy of $I^\pi = 10^- \hbar$ level of the main band. The calculated wavefunction amplitude probabilities from TPSM as a function of spin for the main and the partner bands are shown in (b) and (c), respectively. The numbers quoted in the parenthesis in the box of Fig. 3(b) are the quasi-particle energies in MeV.

Spin $I[\hbar]$	Lifetime [ps]	B(M1) [$(\mu_N)^2$]	B(E2) [$(eb)^2$]
Main Band			
12^-	0.32 (2)	1.22 (1)	0.10 (1)
13^-	0.21 (2)	1.70 (2)	0.10 (1)
14^-	0.25 (2)	0.80 (6)	0.10 (1)
15^-	0.23 (2)	0.45 (7)	0.10 (1)
16^-	0.17 (1)	0.67 (7)	0.09 (1)
17^-	0.12 (1)	1.12 (12)	0.10 (2)
Partner Band			
14^-	1.77 (10)	0.68 (4)	0.13 (1)
15^-	0.31 (1)	2.02 (12)	0.12 (2)
16^-	0.42 (2)	0.49 (3)	0.09 (1)
17^-	0.26 (1)	0.69 (6)	0.12 (1)
18^-	0.09 (1)	1.42 (16)	0.1(2)
19^-	0.11 (1)	0.79 (9)	0.13(2)

TABLE I. The measured lifetimes and the corresponding B(M1) and B(E2) values for the doublet bands of ^{106}Ag .

* Corresponding author: pdatta.ehp@gmail.com

- [1] C. M. Petrache, et al., Nucl. Phys. A 597 (1996) 106.
- [2] K. Starosta, et al., Phys. Rev. Lett. 86 (2001) 971.
- [3] T. Koike, K. Starosta, C. J. Chiara, D. B. Fossan, and D. R. LaFosse, Phys. Rev. C 67 (2003) 044319; A. A. Hecht, et al., Phys. Rev. C 63 (2001) 051302(R); D. Hartley, et al., Phys. Rev. C 64 (2001) 031304(R).
- [4] C. Vaman, et al., Phys. Rev. Lett. 92 (2004) 032501.
- [5] P. Joshi, et al., Phys. Rev. Lett. 98 (2007) 102501.
- [6] P. Joshi, et al., Phys. Lett. B 595 (2004) 135; J. Timar, et al., Phys. Lett. B 598 (2004) 178; P. Joshi, et al., Eur. Phys. J. A24 (2005) 23,
- [7] J. Sethi, et al., Phys. Lett. B 725 (2013) 85.

- [8] V. I. Dimitrov, S. Frauendorf and F. Donau, Phys. Rev. Lett. 84 (2000) 5732.
- [9] S. Frauendorf and J. Meng, Nucl. Phys. A 617 (1997) 131.
- [10] C. M. Petrache, G. B. Hagemann, I. Hamamoto and K. Starosta, Phys. Rev. Lett. 96 (2006) 112502.
- [11] D. Tonev, et al., Phys. Rev. Lett. 96 (2006) 052501.
- [12] S. Mukhopadhyay, et al., Phys. Rev. Lett 99 (2007) 172501.
- [13] S. Mukhopadhyay, et al., Phys. Rev. C 78 (2008) 034311.
- [14] E. Grodner, et al., Phys. Rev. Lett. 97 (2006) 172501.
- [15] H. Ma, et al., Phys. Rev. C 88 (2013) 034322.
- [16] S. H. Yao, et al., Proceedings of 13th National Conference on Nuclear Structure in China (NSC2010) (World Scientific, Singapore, 2011) 271.
- [17] J. A. Sheikh, G. H. Bhat, Y. Sun, G. B. Vakil and R. Palit, Phys. Rev. C 77 (2008) 034313.
- [18] S. Muralithar, et al., Nucl. Instrum. Methods A 622 (2010) 281.
- [19] R. Palit, et al., Nucl. Instrum. Methods A 680 (2012) 90.
- [20] D. C. Radford, Nucl. Instrum. Methods, A 361 (1995) 297.
- [21] J. C. Wells and N. R. Johnson, Oak Ridge National Laboratory Report No. ORNL-6689, (1991) 44.
- [22] L. C. Northcliffe, et al., Nucl. Data, Sect. A7, (1970) 233.
- [23] P. Datta, et al., Phys. Rev. C 69 (2004) 044317.
- [24] S. Roy, et. al., Phys. Lett. B 694 (2011) 322.
- [25] G. H. Bhat, et al, Phys. Lett. B 707 (2012) 250.
- [26] S. Roy, et al., Phys. Lett. B 710 (2012) 587.